

Terrylenediimide: A Novel Fluorophore for Single-Molecule Spectroscopy and Microscopy from 1.4 K to Room Temperature

S. Mais,* J. Tittel, Th. Basché,[†] and C. Bräuchle

Institut für Physikalische Chemie, Universität München, Sophienstrasse 11, 80333 München, FRG

W. Göhde and H. Fuchs

Physikalisches Institut, Universität Münster, Wilhelm-Klemm-Strasse 11, 48149 Münster, FRG

G. Müller and K. Müllen

Max-Planck-Institut für Polymerforschung, Ackermannweg 10, 55128 Mainz, FRG

Received: June 10, 1997[⊗]

The photophysical properties of terrylenediimide (TDI) make this novel fluorophore an ideal candidate for single-molecule studies in solid matrices using various optical techniques. By employing frequency selective high-resolution laser spectroscopy at liquid helium temperatures, we could isolate the fluorescence excitation lines of single TDI molecules. Additionally, vibrational modes of the molecule were examined and the population and depopulation rates of the triplet state determined. At temperatures between 100 K and room temperature single TDI molecules were imaged by confocal fluorescence microscopy. In these investigations one-step irreversible bleaching and “on–off” transitions of the fluorescence were observed.

1. Introduction

The optical detection of single fluorophores in the condensed phase has been achieved by frequency selective as well as microscopic techniques.¹ In single-molecule spectroscopy (SMS) at low temperatures the appearance of sharp zero-phonon lines, the width of which are much narrower than the inhomogeneous broadening of the optical transition, allows the selective addressing of single molecules in frequency space by absorption² or fluorescence excitation³ using dilute samples and tunable, narrow-bandwidth laser sources. When a microscopic technique (near-field or far-field)^{4–6} is used, experimental conditions have to be established allowing one to image only the emission of a single fluorophore—at least on average—in the probe volume defined by the optical resolution of the system. In low-temperature fluorescence microscopy⁷ both techniques were combined, allowing the observation of spatially separated molecules which absorb at different excitation frequencies.

Although they are of crucial importance to research topics such as spectral dynamics in solids or on surfaces,^{8,9} to date no single-molecule studies have been reported where the same molecular system was investigated over an extended temperature range. The measurements were done either at room temperature or at very low temperatures below 10 K. For any form of microscopy used for spatial isolation and imaging of individual fluorophores there is in principle no restriction on the temperature at which the measurement is performed. When doing single-molecule measurements over an extended temperature range, it would be, however, advantageous to study systems exhibiting zero-phonon lines at low temperatures. This then allows for precise, high-resolution spectroscopic studies in the corresponding temperature range, increasing the merits of variable temperature microscopy, which is experimentally more difficult to implement. Combining the knowledge available

from the literature,¹ the ideal fluorophore for this application should have the following main properties: strong absorption, high fluorescence quantum yield, negligible population of bottleneck states, low photobleaching efficiency at room temperature, and weak electron–phonon coupling at low temperature. Especially the latter two requirements are rarely observed simultaneously in the list of fluorophores used for single-molecule studies. Fluorophores such as rhodamine 6G and fluorescein, which were used for room temperature work,^{5,9} do not exhibit zero-phonon lines at low temperature,¹⁰ while aromatic hydrocarbons such as pentacene or terrylene, which were investigated at low temperatures, are known for their poor photostability under ambient conditions.

In this paper we present single-molecule data with terrylenediimide (TDI), a derivative of the aromatic hydrocarbon terrylene. Terrylene^{11–14} and tetra-*tert*-butylterrylene (TBT)¹⁵ were already successfully used in a number of recent low-temperature single-molecule experiments. The novel fluorophore TDI combines to a large extent most of the desired properties for single-molecule studies at various temperatures, as described in the foregoing paragraph. The fairly high photostability allowed single-molecule imaging (in a PVB film) at room temperature using confocal microscopy. We also used this setup to record images at lower temperatures down to 96 K. At 1.4 K we observed sharp zero-phonon lines of single absorbers (in polyethylene or hexadecane) by frequency selective high-resolution laser spectroscopy. Additionally, we recorded vibrationally resolved emission spectra and used fluorescence correlation spectroscopy to determine photophysical parameters of the triplet state. These investigations present the first step toward the future goal of studying the same single fluorophore from liquid helium to room temperature.

2. Experimental Section

TDI, a novel fluorophore, was synthesized according to the literature.¹⁶ The room-temperature absorption spectrum in hexadecane (HD) and the molecular structure of TDI are shown

[†] Present address: Institut für Physikalische Chemie, Johannes Gutenberg-Universität, 55099 Mainz, FRG.

[⊗] Abstract published in *Advance ACS Abstracts*, October 1, 1997.

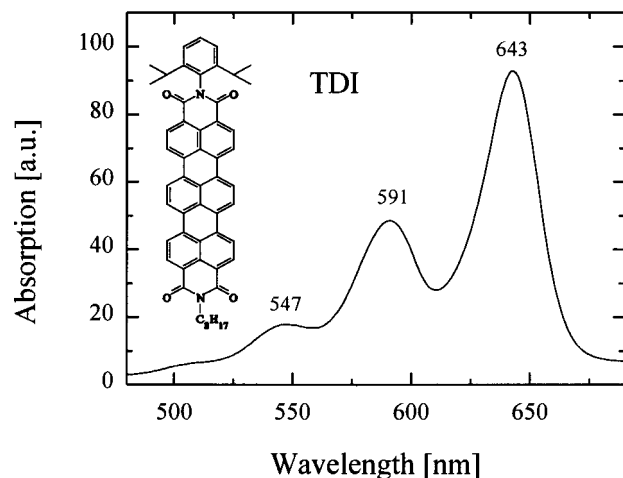


Figure 1. Absorption spectrum of a bulk solution of TDI in HD at room temperature. At 643 nm the maximum extinction coefficient is $93\,000\text{ L mol}^{-1}\text{ cm}^{-1}$. The inset shows the structure of TDI.

in Figure 1. The substituents at the nitrogen atoms serve as protective groups required for the synthesis and also enhance solubility. The absorption maximum appears at 643 nm and the extinction coefficient at this wavelength amounts to approximately $90\,000\text{ L mol}^{-1}\text{ cm}^{-1}$. TDI molecules can be conveniently excited by a HeNe laser, a Kr^+ laser, a DCM dye laser, or even a cheap diode laser.

For the various measurements described below we prepared samples of TDI in different matrices. Thin films of TDI in polyvinylbutyral (PVB) were spin-coated onto a cleaned quartz cover slide from a solution of $1.8 \times 10^{-9}\text{ mol/L}$ TDI and 2 g/L PVB in methylene chloride. The topography of the films has a roughness of less than 5 nm over areas of many square micrometers, as was controlled by atomic force microscopy and topography images obtained with scanning near-field optical microscopy. The thickness of the films was measured to be 20–30 nm by evaluation of the depth of holes which are occasionally present at some sample locations. From the film thickness together with the relation of the concentrations of TDI and PVB in the solution, the concentration of the TDI molecules in the film is calculated to be $12 \pm 6\text{ molecules}/(\mu\text{m}^2 \times 20\text{ nm})$. Polyethylene samples (thickness $\sim 10\ \mu\text{m}$) were prepared by predissolving TDI in methylene chloride, mixing with low-density polyethylene (PE), drying at 300 K under high vacuum, pressing films at 440 K between glass slides, and subsequent quenching to 77 K. To obtain a solution ($c \approx 6 \times 10^{-6}\text{ mol/L}$) of TDI in hexadecane (HD), the chromophore was predissolved in a small amount of methylene chloride. The mixture was then heated to evaporate most of the methylene chloride.

Two different experimental setups were employed in this work. For single-molecule imaging between room temperature and 96 K we used a variable temperature confocal microscope.¹⁷ The $\lambda = 633\text{ nm}$ light of a HeNe laser or the $\lambda = 647\text{ nm}$ light of a Kr^+ laser was focused through a pinhole and reflected to a microscope objective ($60\times$, 0.85) by a beam splitter. The objective focuses the illumination light with typical excitation intensities of 20 kW/cm^2 on-axis into the sample plane. The sample assembly is moved laterally across the focus by a piezoelectric bimorph scanner. Both the objective and the scanner are located inside the optical cryostat. The light collected by the same objective is focused through a second pinhole in the image plane of the objective. The excitation light is suppressed by cutoff filters (Schott RG 665) and the fluorescence emission detected with a photon-counting avalanche photodiode (EG+G, SPCM-200, APD). The output

pulses of the APD were counted for 5–10 ms for each pixel, yielding a total imaging time of 15–30 min.

For frequency selective single-molecule spectroscopy at low temperatures we employed the so-called fiber setup.^{3,18} The light of a single-mode DCM dye laser (Coherent 699-21) is coupled into a polarization-preserving single-mode optical fiber. The samples are mounted directly at the end of this fiber, which itself is fixed at the focus of a parabolic mirror inside a liquid helium cryostat. The TDI/PE films were glued to the fiber by a small amount of adhesive, while a thin layer of TDI/HD was prepared by simply dipping the cleaved fiber end into a solution of TDI in hexadecane and then quickly cooling the wetted fiber inside the cryostat. The light emerging from the sample is collected with the parabolic mirror and directed outside the cryostat. To measure the fluorescence excitation spectrum of single absorbers, the red-shifted fluorescence light is separated from scattered excitation light by a long pass filter (Schott RG 715) and detected as a function of excitation wavelength with a photomultiplier tube and photon-counting electronics. Vibrationally resolved fluorescence spectra of single TDI molecules were recorded by tuning the laser in resonance with the molecular transition, dispersing the emission with a spectrograph (Jobin Yvon HR460), and imaging on a liquid nitrogen cooled CCD camera (Princeton). Typical acquisition times were 300 s at a spectral resolution of $\sim 5\text{ cm}^{-1}$. To acquire the fluorescence correlation function which was also measured at a fixed excitation frequency, the photoelectric pulses from the PMT were fed into a digital logarithmic correlator (ALV5000) with time resolution $< 1\ \mu\text{s}$. The excitation intensity was varied from 40 mW/cm^2 to 6.4 W/cm^2 in these measurements.

3. Results and Discussion

3.1. Confocal Microscopy at Room Temperature and 96 K.

A confocal image of TDI molecules in a thin PVB film taken at room temperature is shown in Figure 2a. The size of the spots corresponds to a microscopic resolution of $\sim 1\ \mu\text{m}$, which is achieved with the objective. The high photostability of the molecules, even at room temperature, allows a repeated imaging of similar patterns for long time periods. Some of the spots in the image instantaneously disappeared while scanning. This one-step bleaching is characteristic for single-molecule fluorescence.^{9,19} From this behavior and the low concentration of the dye molecules we are sure that each spot, if not overlapping with another, corresponds to the fluorescence light from a single molecule.

Using the low-temperature ability of our instrument,¹⁷ we also took a series of three images at $T = 96\text{ K}$, presented in Figure 2b. Each image requires 30 min of recording time. The reduced count rates are attributed to a different excitation wavelength of $\lambda = 647\text{ nm}$. As compared to room-temperature measurements with the same laser, however, the fluorescence signal does not show an increase. In the repeated scans of Figure 2b over the same area bleaching of single molecules is observed (e.g. arrow A). Even more interestingly, another spot (arrow B), which is not visible in the first image, appears in the second and third image. The disappearance and reappearance (“off–on” transitions)²⁰ of single-molecule fluorescence over a long time period is directly visible in Figure 2c, which shows the variation of fluorescence intensity with time for three different sample locations not far away from the region of Figure 2b. In Figure 2c-i an average rate of 300 counts per 100 ms above the background was collected before one-step bleaching occurs at the time $t_a = 50\text{ s}$. These 150 000 counts before bleaching correspond to a total fluorescence photon yield of $\sim 10^7$, taking into account the estimated detection efficiency of 1–2%.¹⁷ In

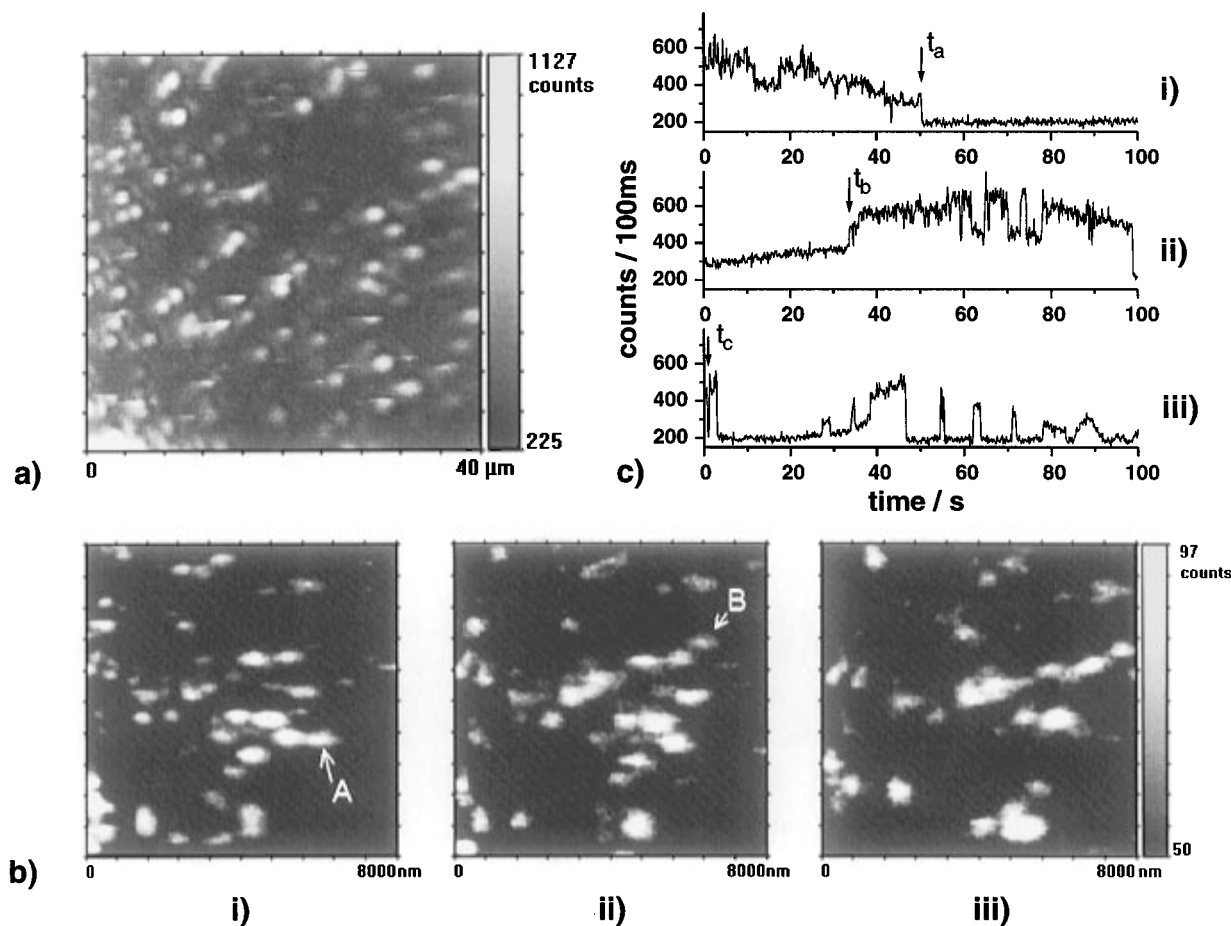


Figure 2. (a) Room-temperature confocal fluorescence image of TDI in a ~ 25 nm thin PVB film on quartz. Excitation intensity: 30 ± 10 kW/cm² at $\lambda = 633$ nm. Integration time per pixel: 5 ms. The scan direction is from left to right and bottom to top. Some spots instantaneously disappear while scanning over the molecules. Note also the black stripes on some spots, appearing due to an “on–off–on” transition of the fluorescence during the scan. (b) Section from a series of three fluorescence images of the same area at $T = 96$ K. Excitation: 20 kW/cm² at $\lambda = 647$ nm. Time per pixel: 10 ms. In the second image molecule A disappeared. Molecule B, not visible in the first image, appears in the second and third image. The data sets were filtered by a 3×3 convolution kernel. Note: During recording of the data the whole image shifted from left to right. (c) 100 s traces of the fluorescence at three different sample locations near the imaged area of b, recorded at $T = 96$ K. They show different behaviors such as one-step bleaching (i), sudden increase (ii), and “on” and “off” switching (iii) of the fluorescence (see text).

Figure 2c-ii the fluorescence signal of a molecule appears at time t_b , 33 s after starting the illumination, and undergoes a number of short transitions before disappearing just before the end of the observation period of 100 s. In Figure 2c-iii the signal of the investigated molecule instantaneously reappears at t_c after a temporary “off” state. Over a time of 100 s the same molecule switches “on” and “off” repeatedly, reaching different fluorescence levels. Besides instantaneous jumps of the fluorescence intensity, quite fast continuous changes can be observed as well. As molecular reorientations can be excluded in this temperature range and experimental drifts cause only slow variations, these might originate from spectral shifts^{21–23} or from fast “on–off” transitions with a slowly varying relation of the average “on” and “off” times, which are not resolved within the 100 ms counting intervals used here.

These microscopic observations on a single-molecule level reveal inhomogeneities which cannot be resolved by ensemble measurements. Results obtained at room temperature give more quantitative insights into the molecular bleaching process.²⁴ In current experiments we investigate the reason for the repeated “on–off” transitions, which could be spectral jumps of several nanometers due to a reorientation of the molecule’s substituents.

3.2. High-Resolution Spectroscopy at Liquid Helium Temperatures. Fluorescence excitation spectra of single TDI molecules were easily observed in polyethylene (PE) as well as in hexadecane (HD). In the polymeric host, however, the

vast majority of the excitation lines showed spontaneous and/or light-induced frequency jumps²⁵ even when scanning the laser with fairly low intensity. This effect is expected to be also common in PVB samples, which for the present were not investigated in the low-temperature experiments. In the polycrystalline HD matrix the stability of the excitation lines was much better. The hexadecane molecules seem to offer more stable surroundings around the guest molecules, although in the bulk fluorescence excitation spectrum of TDI/HD at 1.4 K only a broad inhomogeneous band with no well-defined Shpol’skii sites is visible. This is quite reasonable taking into account the bulky substituents of TDI, which will not allow for a substitutional insertion into the alkane host, and the likely presence of traces of methylene chloride. All the single-molecule data described in the following were taken in the system TDI in HD.

Single-molecule excitation lines of TDI in HD were observed in the wavelength range between 651 and 668 nm (see Figure 3). All line shapes could be approximated by Lorentzians, one example of which is shown in the inset of Figure 3. The narrowest lines have a full width at half-maximum of around 45 MHz at low exciting intensity (25 mW/cm²). If this corresponds to the lifetime-limited value, the excited-state lifetime, which to our knowledge has not yet been determined by time-resolved measurements, would be 3.5 ns, very similar to the value obtained for terrylene.²⁶ For a few molecules it

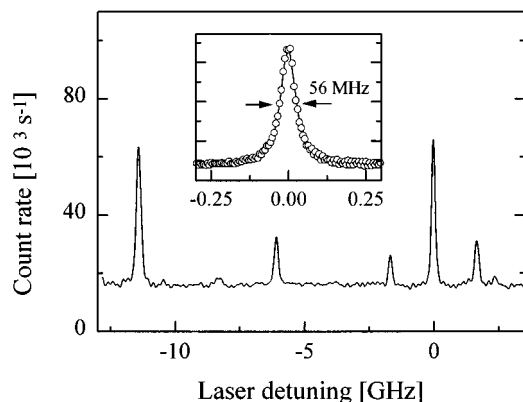


Figure 3. Fluorescence excitation spectrum of single TDI molecules in hexadecane at 1.4 K ($I = 80 \text{ mW/cm}^2$, $0 \text{ GHz} \equiv 659.02 \text{ nm}$). The inset shows the spectrum of one of the molecules together with a Lorentzian fit (solid line; $\Delta\nu_{\text{fwhm}} = 56 \text{ MHz}$).

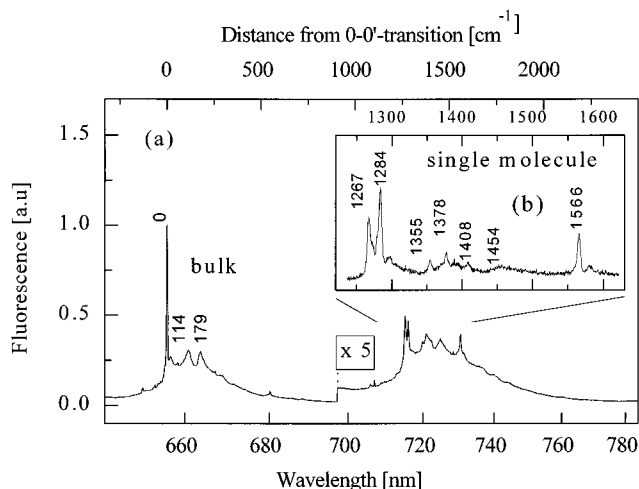


Figure 4. (a) Fluorescence spectrum of a bulk sample of TDI in PE at 1.4 K, excited at 633 nm. (b) Fluorescence spectrum of a single TDI molecule in HD at 2.5 K, excited at its 0–0 transition at 656.13 nm. The vibronic lines are more clearly visible due to the reduced pseudophonon sidebands.

TABLE 1: Vibrational Frequencies in cm^{-1} of TDI in Polyethylene at 1.4 K (the Resolution Is about 5 cm^{-1})

frequency	frequency	frequency
19	547 ^a	1378
59	1082	1405
114 ^a	1104	1454
179 ^a	1267 ^a	1523
257	1283 ^a	1562 ^a
297	1360	

^a Strongest features in the emission spectrum.

was possible to increase the exciting intensity up to 6 W/cm^2 . The line shapes broadened as expected from theory,²⁷ and we reached fluorescence count rates up to $400\,000 \text{ s}^{-1}$ under these conditions.

In Figure 4a the fluorescence line narrowing (FLN) spectrum of a bulk sample of TDI in PE at 1.4 K is plotted. It is seen that a large fraction of the emission intensity is concentrated in the 0,0 transition and that only a small number of vibronic transitions can be discerned. The ground-state vibrational frequencies determined from the emission spectrum are listed in Table 1. Comparison of the emission spectra of TDI and unsubstituted terrylene^{18,28} reveals fairly good agreement of the frequencies of the strong vibronic lines in the fingerprint region (TDI: 1267 cm^{-1} , 1284 cm^{-1} , 1562 cm^{-1} ; terrylene: 1272 cm^{-1} , 1283 cm^{-1} , 1562 cm^{-1}). According to quantum chemical

calculations for terrylene,¹⁸ the corresponding normal vibrations are attributed to C–C stretches, which obviously are only weakly affected by the substituents of TDI. Additionally, the weaker lines at 547 , 1360 , and 1378 cm^{-1} appear at similar frequencies in the spectrum of terrylene. The line at 179 cm^{-1} might correspond to the intense line appearing at 243 cm^{-1} in the terrylene spectrum. This mode is attributed to a long axis stretch of the whole molecule,¹⁸ the vibrational frequency of which is expected to decrease in TDI because of its increased vibrational mass.

As has been mentioned above, in the PE host the single-molecule lines are subject to light-induced frequency jumps. Therefore, it was not possible to excite a TDI molecule resonantly for a sufficiently long time interval to accumulate its emission spectrum. Because of the increased stability, single-molecule fluorescence spectra could be recorded in the HD host. Figure 4b shows the fingerprint region ($1250\text{--}1620 \text{ cm}^{-1}$) of the emission spectrum of a single TDI molecule in HD excited at 656.13 nm . It exhibits the same vibronic pattern as the bulk spectrum of TDI in PE (Figure 4a). Within the experimental resolution (5 cm^{-1}), the spectra of other single TDI molecules investigated show the same vibronic frequencies in this wavelength range. However, we observed clear changes in the intensity ratio between the modes at 1267 and 1284 cm^{-1} for different molecules. For some molecules the intensities of these modes are equal, for some the lower frequency mode is stronger, or vice versa. Interestingly, the intensity ratio of the 1271 and 1283 cm^{-1} modes of single terrylene molecules (in PE) was also found to vary considerably between different molecules.¹⁸ The authors of ref 18 suggested that these modes may be especially sensitive to small distortions of the terrylene skeleton or variations in the local environment, as corroborated by quantum chemical calculations. Additionally, a slight degree of correlation was found between the intensity ratio of these modes and the excitation frequency. In our study of single TDI molecules such a correlation was not observed, but the number of molecules investigated may be too small.

The fluorescence intensity autocorrelation function $g^{(2)}(\tau)$ ²⁹ was recorded to determine the population and depopulation rates of the triplet state of single TDI molecules. These parameters can be deduced from the time constant and the contrast of the decay visible in the correlation function. This decay is a well-known phenomenon resulting from bunching of the fluorescence photons caused by singlet–triplet quantum transitions.³⁰ To extract the kinetic parameters of the triplet state from the correlation decay, intensity dependent measurements have to be performed. From the more than 100 single molecules examined only two endured this procedure because at high excitation intensity light-induced frequency changes occurred. These two molecules showed three steps in the time regions of 0.1, 1, and 100 ms when plotting the correlation function on a logarithmic time scale (see Figure 5a). Hence the correlation function was approximated by the sum of three exponentials.

$$g^{(2)}(\tau) = 1 + c_1 \exp(-\lambda_1 \tau) + c_2 \exp(-\lambda_2 \tau) + c_3 \exp(-\lambda_3 \tau) \quad (1)$$

As will be explained later, the exponential decay around 100 ms could not be attributed to triplet dynamics but rather seems to be due to spectral diffusion. The first two exponential decays of the correlation function are thought to be caused by intersystem crossing (ISC) into and out of the triplet state of TDI. As the main molecular frame forming the π system is expected to be close to planarity, we assume in analogy to terrylene¹⁴ that the fast decay ($i = 1$) is due to the two in-plane sublevels, the contributions of which cannot be discriminated

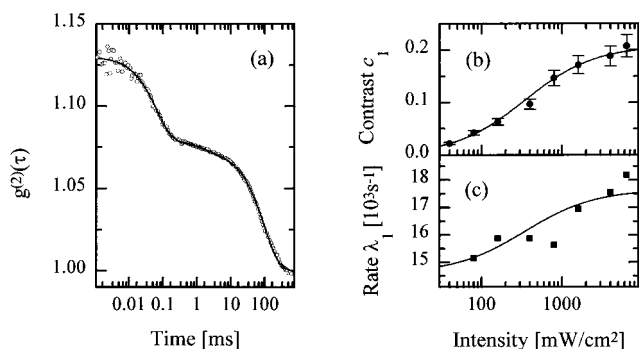


Figure 5. (a) Normalized intensity autocorrelation function $g^{(2)}(\tau)$ of the fluorescence emission of a single TDI molecule at an excitation intensity of 0.8 W/cm^2 . The solid line is a fit of three exponentials (eq 1) to the experimental data, yielding decay times of $\lambda_1^{-1} = 66 \mu\text{s}$, $\lambda_2^{-1} = 1.7 \text{ ms}$, and $\lambda_3^{-1} = 101 \text{ ms}$. The second step is hardly visible but necessary to obtain a satisfying fit. Background-corrected contrasts (b) and rates (c) of the first exponential decay in $g^{(2)}(\tau)$ of a single TDI molecule versus exciting laser intensity (note the logarithmic intensity axis). The behavior can be well reproduced with the theory described in ref 30 (solid lines). The error of the contrast is assumed to be less than 10%. The fits yield $k_{23}^{(1)} = 6.1 \text{ ms}^{-1}$ and $k_{31}^{(1)} = 14.6 \text{ ms}^{-1}$.

TABLE 2: Average ISC Rates $k_{23}^{(i)}$ and $k_{31}^{(i)}$ of Two TDI Molecules in Hexadecane As Determined from the Intensity Dependence of the Correlation Decay Rates and Contrasts (See Figure 5 and Text)

	(1)	(2)
$k_{23} (10^3 \text{ s}^{-1})$	5 ± 2	< 1
$k_{31} (10^3 \text{ s}^{-1})$	15 ± 1	1.5 ± 1

in our experiments, and the slow decay ($i = 2$) is due to the out-of-plane sublevel.

For the determination of the ISC rates we treated the sublevel populations in a first approximation as if they were independent using the formalism of ISC in a three-level system.³⁰ When we included coupling of sublevel populations in the rate equations, as recently shown in ref 31, we found the deviation of the rate parameters to be within our experimental error margin. The rate parameters λ_i ($i = 1, 2$) and the contrasts c_i (corrected for background contributions according to eq 12 of ref 30) of the correlation function depend on the intensity and are related to the population ($k_{23}^{(i)}$) and depopulation rates ($k_{31}^{(i)}$) of the triplet state as given in eqs 7 and 10 of ref 30. It is, in principle, possible to determine the values of $k_{23}^{(i)}$ and $k_{31}^{(i)}$ from the rate parameters λ_i alone, but the analysis of the contrasts c_i additionally provides the ratio $k_{31}^{(i)}/k_{23}^{(i)}$, which helps to arrive at more precise results. A plot of c_1 and λ_1 versus I is shown in Figure 5b,c, together with the corresponding fits. From the fitting procedure we obtained $k_{23}^{(1)} = 6.1 \text{ ms}^{-1}$ and $k_{31}^{(1)} = 14.6 \text{ ms}^{-1}$. The analysis of the second exponential decay was not possible in the same way because the contrast c_2 was extremely low. We were only able to determine $k_{31}^{(2)}$, which at low intensities approaches λ_2 , and set an upper limit for $k_{23}^{(2)}$. In Table 2 the average population and depopulation rates of two molecules are summarized. As was also found for terrylene, the population rates of the triplet state, which themselves are many orders of magnitude smaller than the fluorescence rate, are smaller than the depopulation rates. These results account for a weak triplet population and strong fluorescence emission in TDI.

The intensity dependence of the true contrast of the exponential decay c_3 at long times (see Figure 5a) shows a completely different behavior as predicted for singlet-triplet transitions, because it vanishes at high intensities. We assume the decay around 100 ms to originate from light-induced spectral diffusion.³² A single two-level system (TLS) in the vicinity of the

molecule causes a second absorption frequency to be visited, which also introduces bunching of photons. An indication of this second frequency position is found in the fluorescence excitation spectrum at higher intensities. Two line shapes are visible showing discrete interruptions of the signal when the molecule is visiting the other frequency position. For even higher intensities power broadening causes merging of the two spectral lines. Consequently, the fluorescence intensity is constant and independent of the state of the TLS, and the related contrast vanishes.³² Strangely, this behavior was found qualitatively quite similar for both molecules.

4. Conclusion

Terrylenediimide was introduced as a suitable fluorophore for single-molecule imaging and spectroscopy in the wide temperature range from 1.4 K to room temperature. It combines the essential properties of strong and sharp zero-phonon lines at low temperature and a sufficient photostability at room temperature. With the variable temperature confocal microscope we studied fluorescence dynamics of the single chromophores in a solid matrix and observed fluctuations and “blinking” behavior of the fluorescence at 96 K and room temperature. A similar phenomenon, well-known in low-temperature single-molecule spectroscopy as spectral diffusion, was observed by high-resolution laser spectroscopy as well. Actually, for many examinations spectral diffusion is rather a disturbing effect connected with the complex structure of the dye molecule which prevents an ordered nanoenvironment. Nevertheless, it was possible to record single-molecule fluorescence spectra at 1.4 K and to determine the ISC rates of TDI.

The results obtained so far promise interesting future investigations over a broad temperature range. Avoiding ensemble averaging, it seems to be possible to reach a detailed understanding of the “blinking” behavior. The special design of the molecule also allows chemical modifications which may be useful to study specific dye-matrix interactions. Furthermore, it will be possible to attach TDI to polymer chains or biomolecules or to covalently connect two dye molecules directly for energy or electron-transfer experiments at the single-molecule level.

Acknowledgment. We would like to thank R. Kettner and F. Kulzer for measuring the fluorescence spectrum of TDI/PE. Financial support by the Deutsche Forschungsgemeinschaft and the Fonds der Chemischen Industrie is gratefully acknowledged.

References and Notes

- (1) Basché, T.; Moerner, W. E.; Orrit, M.; Wild, U. P., Eds. *Single-Molecule Optical Detection, Imaging and Spectroscopy*; VCH: Weinheim, 1997.
- (2) Moerner, W. E.; Kador, L. *Phys. Rev. Lett.* **1989**, *62*, 2535.
- (3) Orrit, M.; Bernard, J. *Phys. Rev. Lett.* **1990**, *65*, 2716.
- (4) Betzig, E.; Chichester, R. J. *Science* **1993**, *262*, 1422.
- (5) Nie, S.; Chiu, D. T.; Zare, R. N. *Science* **1994**, *266*, 1018.
- (6) Eigen, M.; Rigler, R. *Proc. Natl. Acad. Sci. U.S.A.* **1994**, *91*, 5740.
- (7) Jasny, J.; Sepiol, J.; Irngartinger, T.; Traber, M.; Renn, A.; Wild, U. P. *Rev. Sci. Instrum.* **1996**, *67*, 1425.
- (8) Skinner, J. L.; Moerner, W. E. *J. Phys. Chem.* **1996**, *100*, 13251.
- (9) Ambrose, W. P.; Goodwin, P. M.; Martin, J. C.; Keller, R. A. *Phys. Rev. Lett.* **1994**, *72*, 160.
- (10) McColgin, W. C.; Marchetti, A. P.; Eberly, J. H. *J. Am. Chem. Soc.* **1978**, *100*, 5622.
- (11) Orrit, M.; Bernard, J.; Zumbusch, A.; Personov, R. I. *Chem. Phys. Lett.* **1992**, *196*, 595.
- (12) Tchenio, P.; Myers, A. B.; Moerner, W. E. *J. Lumin.* **1993**, *56*, 1.
- (13) Moerner, W. E.; Plakhotnik, T.; Irngartinger, T.; Croci, M.; Palm, V.; Wild, U. P. *J. Phys. Chem.* **1994**, *98*, 7382.
- (14) Kummer, S.; Basché, Th.; Bräuchle, C. *Chem. Phys. Lett.* **1994**, *229*, 309; **1995**, *232*, 414.

- (15) Tittel, J.; Kettner, R.; Basché, Th.; Bräuchle, C.; Quante, H.; Müllen, K. *J. Lumin.* **1994**, *64*, 1.
- (16) Holtrup, F.; Müller, G.; Quante, H.; De Freyter, S.; De Schryver, F. C.; Müllen, K. *Chem. Eur. J.* **1997**, *3*, 219.
- (17) Göhde, W.; Tittel, J.; Basché, Th.; Bräuchle, C.; Fischer, U. C.; Fuchs, H. *Rev. Sci. Instrum.* **1997**, *68*, 2466.
- (18) Myers, A. B.; Tchénió, P.; Zgierski, M. Z.; Moerner, W. E. *J. Phys. Chem.* **1994**, *98*, 10377.
- (19) Xie, X. S.; Dunn, R. C. *Science* **1994**, *265*, 361.
- (20) Trautman, J. K.; Macklin, J. J. *J. Chem. Phys.* **1996**, *205*, 221.
- (21) Trautman, J. K.; Macklin, J. J.; Brus, L. E.; Betzig, E. *Nature* **1994**, *369*, 40.
- (22) Ha, T.; Enderle, Th.; Chemla, D. S.; Selvin, P. R.; Weiss, S. *Phys. Rev. Lett.* **1996**, *77*, 3979.
- (23) Lu, H. P.; Xie, X. S. *Nature* **1997**, *385*, 143.
- (24) Göhde, W.; Tittel, J.; Basché, Th.; Bräuchle, C.; Fischer, U. C.; Fuchs, H.; Müller, G.; Müllen, K. To be published.
- (25) Basché, Th.; Moerner, W. E. *Nature* **1992**, *355*, 335.
- (26) Plakhotnik, T.; Moerner, W. E.; Irgartinger, T.; Wild, U. P. *Chimia* **1994**, *48*, 31.
- (27) Ambrose, W. P.; Basché, Th.; Moerner, W. E. *J. Chem. Phys.* **1991**, *95*, 7150.
- (28) Tchenio, P.; Myers, A. B.; Moerner, W. E. *Chem. Phys. Lett.* **1993**, *213*, 325.
- (29) Loudon, R. *The Quantum Theory of Light*, 2nd ed.; Oxford University Press: Oxford, 1983.
- (30) Bernard, J.; Fleury, L.; Talon, H.; Orrit, M. *J. Chem. Phys.* **1993**, *98*, 850.
- (31) Boiron, A.-M.; Lounis, B.; Orrit, M. *J. Phys. Chem.* **1996**, *105*, 3969.
- (32) Fleury, L.; Zumbusch, A.; Orrit, M.; Brown, R.; Bernard, J. *J. Lumin.* **1993**, *56*, 15.